1   Title page

2   **Cortical entrainment to hierarchical contextual rhythms**

3   **recomposes dynamic attending in visual perception**

4   Peijun Yuan[1, 2], Ruichen Hu[1, 2], Xue Zhang[1, 2], Ying Wang[1, 2]*, Yi Jiang[1, 2]*

5   [1]State Key Laboratory of Brain and Cognitive Science, CAS Center for Excellence in Brain

6   Science and Intelligence Technology, Institute of Psychology, Chinese Academy of Sciences,

7   16 Lincui Road, Beijing 100101, P. R. China

8   [2]Department of Psychology, University of Chinese Academy of Sciences, 19A Yuquan Road,

9   Beijing 100049, P. R. China

10   *For correspondence: wangying@psych.ac.cn; yijiang@psych.ac.cn

11

Abstract

12

13   Temporal regularity is ubiquitous and essential to guiding attention and coordinating

14   behavior within a dynamic environment. Previous researchers have modeled attention as

15   an internal rhythm that may entrain to first-order regularity from rhythmic events to

16   prioritize information selection at specific time points. Using the attentional blink

17   paradigm, here we show that higher-order regularity based on rhythmic organization of

18   contextual features (pitch, color, or motion) may serve as a temporal frame to recompose

19   the dynamic profile of visual temporal attention. Critically, such attentional reframing

20   effect is well predicted by cortical entrainment to the higher-order contextual structure at

21   the delta band as well as its coupling with the stimulus-driven alpha power. These results

22   suggest that the human brain involuntarily exploits multiscale regularities in rhythmic

23   contexts to recompose dynamic attending in visual perception, and highlight neural

24   entrainment as a central mechanism for optimizing our conscious experience of the world

25   in the time dimension.

26

Introduction

28 Deploying attention over time is crucial for guiding human activities within a rapidly

29 changing environment. However, the constant influx of information goes far beyond our

30 mental capacity, impeding even the most competent human brain from capturing every

31 nuance of the details. How does the human brain surmount such limitations in temporal

32 attention allocation during dynamic information processing?

33 One feasible solution, as that for spatial attention, is through selection, or by shining

34 an attentional "spotlight" on the most relevant information while filtering out the

35 irrelevant regarding the task demands (Posner, 1980). When it comes to the temporal

36 domain, people tend to utilize regularities in the sensory information flow for directing

37 attention to the moments when a target event is expected to occur (Nobre et al., 2007;

38 Nobre & van Ede, 2018). As a great example, Jones and colleagues have shown in a series

39 of studies that after listening to a rhythmic tone sequence, auditory perception in terms

40 of pitch judgment and time discrimination was more accurate for target tones appearing

41 at the expected than the unexpected time points (Jones et al., 2002; Large & Jones, 1999).

42 Such facilitation effects have been extended to various aspects of visual perception and

43 even across sensory modalities (Bolger et al., 2014; Brochard et al., 2013; Mathewson et

44 al., 2010; Miller et al., 2013; ten Oever et al., 2014), implicating the involvement of a

45 general attentional selection mechanism guided by the regularity in stimulus timing.

46 In this line of studies, perceptual responses were significantly improved for targets

47 appearing within a rhythmic context but not within an arrhythmic context. These findings

48 can be interpreted by the dynamic attending theory (DAT), which assumes attention as an

49 internal oscillatory activity (or attending rhythm) that can be entrained to rhythmic

50 structures of the exogenous events (Jones, 1976; Jones et al., 1981; Jones & Boltz, 1989;

51 Large & Jones, 1999). In line with this assumption, electrophysiological research in

52 humans and non-human primates have found entrainment of intrinsic neural oscillations

53 to external stimulus rhythms, and regarded such process as an instrument for selective

54 attention (Calderone et al., 2014; Obleser & Kayser, 2019; Schroeder & Lakatos, 2009).

55 Through neural entrainment, neuronal excitability aligns with the occurrence of rhythmic

56 events, creating "temporal attentional spotlights" that attract the brain's attentional

57 resources towards a string of selected moments (Calderone et al., 2014; Henry &

58 Herrmann, 2014; Lakatos et al., 2008, 2013; Schroeder & Lakatos, 2009).

59   The synchronization between the internal attending rhythm and the external

60 rhythms allows us to direct attention proactively and enhance perception at the

61 anticipated moments. With regards to forming a coherent perception of the dynamic

62 environment, however, we should not only select information bound to the anticipated

63 time points, but also allocate attentional resources among these points, raising the

64 problem of dynamic attentional deployment over an information stream. For instance,

65 when viewing a rapid serial visual presentation (RSVP) stream, there is a large chance that

66 the observer would miss the second of two temporally proximate targets, as the allocation

67 of attention to the first target hinders the redeployment of mental resources to the second

68 one (Broadbent & Broadbent, 1987). This phenomenon, vividly referred to as the

69 attentional blink (AB)(Chun & Potter, 1995; Raymond et al., 1992), has attracted much

70 interest as it reveals the limitations of attentional allocation and memory processes that

71 may become a bottleneck for conscious awareness (Dux & Marois, 2009; Martens & Wyble,

72 2010; Shapiro et al., 1997). More intriguingly, as items in the RSVP stream are all

73 rhythmically presented and temporally predictable, the AB effect poses a challenge in

74 dynamic attending that cannot be circumvented solely by the anticipation built upon

75 stimulus timing.

76   To address this challenge, here we propose that, the brain has to rely, as a

77 complement to the first-order regularity in rhythmic stimulation, on regularities in the

78 higher-order temporal structure of the information stream. More specifically, if the

79 endogenous attentional rhythm could entrain automatically not only to the stimulus

80 rhythm but also to the higher-order structure based on the information content, the

81 deployment of temporal attention might be reconstructed in a way that facilitates target

82 detection in the AB task. To test this hypothesis, we synchronized the original AB stream

83 (stimulation rate at 10 Hz) to a hierarchical contextual stream that possessed a feature-

84 based temporal structure—a 2.5Hz rhythm arising from periodic changes of a physical

85 feature, superimposed on its stimulus rhythm at 10Hz. Using temporal structures defined

4

86 by a variety of features (pitch, color, etc.), we provided converging evidence that the

87 structured context, which was task-irrelevant and even from a different modality, could

88 regulate the dynamic deployment of visual attention so as to alleviate the AB effect. To

89 further unravel the neural basis of the observed attentional modulation effect, we

90 conducted an electroencephalogram (EEG) experiment. We are particularly interested in

91 whether neural oscillations can entrain to the contextual temporal structure of stimulus

92 feature along with that of stimulus onset timing, and more critically, whether and how the

93 cortical entrainment to these hierarchical structures mediates the behavioral modulation

94 effect.

Results

Temporal structure of contextual auditory stream recomposes visual attentional deployment

98 In Experiment 1a, we first explored whether feature-defined temporal structure from a

99 contextual auditory stream could regulate visual attentional deployment during the AB

100 task. If so, the AB effect should be modulated by the positions of the visual targets relative

101 to the rhythmic structure arising from periodic changes of the background sounds (Fig.

102 1A). Above all, we found a robust AB effect in the short-SOA conditions, no matter whether

103 there were contextual sounds or not. The T2 detection accuracy conditioned on correct

104 T1 response was generally impaired in the short-SOA conditions relative to that in the

105 long-SOA condition, during both the context session (long-SOA: 0.945 ± 0.016 (mean ± se),

106 short-SOA: 0.728 ± 0.034, $t(15)$ = 5.443, p < .001, Cohen's d = 1.361) and the baseline

107 session (long-SOA: 0.950 ± 0.013, short-SOA: 0.702 ± 0.034, $t(15)$ = 6.720, p < .001,

108 Cohen's d = 1.680).

109 More importantly, looking close at T2 performance in the short-SOA conditions (Fig.

110 1B), we found T2 was better identified when two targets appeared in two adjacent cycles

111 (between-cycle condition) than within the same cycle defined by the background sounds

112 (within-cycle condition). Notably, such difference was observed only for the context

113 session ($t(15)$ = 2.947, p = .010, Cohen's d = 0.737) but not for the baseline (no sound)

114 session ($t(15)$ = -0.212, p = .835, Cohen's d = 0.053), although the target positions were

115   completely matched between these two sessions. Meanwhile, only in the between-cycle

116   condition, the contextual sounds enhanced T2 detection accuracy relative to the baseline

117   ($t(15) = 2.287$, $p = .037$, Cohen's $d = 0.572$), while in the within-cycle condition, the

118   performance kept comparable between the context and baseline sessions ($t(15) = -0.271$,

119   $p = .790$, Cohen's $d = 0.068$). The observed dissociation was further confirmed by a two-

120   way repeated-measures ANOVA, which yielded a significant interaction between

121   experimental session (baseline vs. context session) and target position (between- vs.

122   within-cycle, defined by the context) ($F(1, 15) = 7.151$, $p = .017$, $\eta_p^2 = .323$).

123   Results from Experiment 1a demonstrated that feature-based temporal structure of

124   an auditory stream, though being task-irrelevant, could systematically modulate the

125   allocation of visual attention over the AB stream. Since the temporal structure of the

126   contextual sounds was defined by periodic change of pitch, when two targets were located

127   in distinct cycles as in the between-cycle condition, they were accompanied by different

128   tones, in contrast to that when located within the same cycle they were accompanied by

129   the same tone. It is possible that the contrast of physical stimulation (i.e., pitch) at T1 and

130   T2 could account for the performance improvement in the between-cycle condition. To

131   test this possibility, in Experiment 1b, we matched the pitch of tones at target occurrence

132   with that in Experiment 1a for the between- and within-cycle condition respectively,

133   whereas disrupted feature-based regularity in the temporal structure of the contextual

134   sound sequence (Fig. 1A, bottom). Despite that the sounds paired with the targets were

135   exactly the same as in Experiment 1a, the difference in T2 detection accuracy caused by

136   the contextual sounds was no longer observed ($t(15) = 0.433$, $p = .671$, Cohen's $d = 0.108$),

137   neither was its interaction with experimental session ($F(1, 15) = 2.734$, $p = .119$, $\eta_p^2 = .154$;

138   Fig. 1C). In other words, T2 was identified with similar accuracy across all the conditions

139   in Experiment 1b, suggesting that it is the temporal structure of the contextual sounds,

140   not the pitch difference at target presentation, that accounts for the between-cycle

141   facilitation effect observed in Experiment 1a.

142

Generalization of the modulation effect to different cycle frequencies

In Experiment 1a, the auditory context always changed its pitch value every four items, i.e., every 400 ms as one cycle, resulting in rhythmic cycles at 2.5 Hz. In Experiment 1c, we tested whether the modulation effect we observed could be generalized to other cycle frequencies. We set the pitch change rate to 2 Hz (i.e., five items per cycle; Fig. 2A, upper) and 3.3 Hz (i.e., three items per cycle; Fig. 2A, lower). For both context frequencies, the T2 detection performance in the between-cycle condition was significantly higher than that in the within-cycle condition (Fig. 2B; for 2 Hz, $t(15) = 3.478$, $p = .004$, Cohen's $d = 0.869$; for 3.3 Hz, $t(15) = 2.467$, $p = .030$, Cohen's $d = 0.617$), suggesting successful attentional modulation effects. Furthermore, a repeated-measures ANOVA on T2 accuracy revealed only a significant main effect of relative target position (i.e., between- vs. within-cycle) ($F(1, 15) = 23.320$, $p < .001$, $\eta_p^2 = .609$), with a marginally significant main effect of frequency ($F(1, 15) = 4.337$, $p = .055$, $\eta_p^2 = .224$) and no interaction between these two factors ($F(1, 15) = 0.204$, $p = .658$, $\eta_p^2 = 0.013$).

The effect of temporal attention rather than perceptual grouping

As temporal structure of the context was constructed by auditory items sharing the same feature (i.e., pitch), one may argue that perceptual grouping on the basis of similarity (Bregman, 1994), instead of dynamic attending guided by feature-based temporal regularities, contributes to the between-cycle benefit that we observed. To disentangle these factors, in Experiment 1d, we changed the pitch value of tone sequences irregularly to form auditory streams that could be grouped in varying lengths (Fig. 2C, upper). Though temporal grouping was reserved in this setting, no facilitation effect was observed when targets were separated in two distinct groups relative to when they were displayed within the same group (Fig. 2D, Irreg-G). T2 detection performance was comparable in the between- and the within-group conditions ($t(15) = 0.348$, $p = .733$, Cohen's $d = 0.087$).

Compared with Experiments 1a and 1c, the strength of temporal grouping in Experiment 1d might be attenuated due to irregular number of items in each group, which could lead to the lack of behavioral modulation effect. To solve this issue, in Experiment 1e (Fig. 2C, lower), we changed the pitch every four items to keep the rule of temporal

172 grouping exactly the same as that in Experiment 1a. Nevertheless, we disrupted the

173 regularity of stimulus timing. Such manipulation would have a detrimental impact on

174 dynamic deployment of temporal attention in general, according to the basic assumption

175 of the DAT (Jones et al., 1982; Jones & Boltz, 1989; Large & Jones, 1999). On the other hand,

176 it would have little influence on the grouping effect. Therefore, if temporal attention rather

177 than perceptual grouping is essential to the behavioral modulation effect observed in the

178 current study, we should expect such effect to disappear in Experiment 1e. In line with our

179 speculation, when the stimulus onset timing was randomized, T2 detection performance

180 in the between-cycle condition was no longer improved relative to the within-cycle

181 condition (Fig. 2D, Irreg-T; $t(15) = 0.302$, $p = .767$, Cohen's $d = 0.076$), despite the potential

182 benefit of the grouping effect. Putting together, the absence of context-induced

183 modulation effect in Experiments 1d and 1e consistently supports the idea that temporal

184 grouping without dynamic attending guided by feature- and timing-related regularities in

185 the auditory context is insufficient to cause the behavioral modulation effect.

186 **Temporal regularities in color-defined rhythmic structure recompose visual**
187 **attentional deployment**

188 Information from the auditory modality, like speech and music, is inherently organized in

189 time and provides rich sources of rhythmic structures that can be proactively tracked by

190 the human brain (Arnal & Giraud, 2012; Doelling & Poeppel, 2015; Haegens & Zion

191 Golumbic, 2018; Zion Golumbic et al., 2012). This suggests a possibility that the role of

192 rhythmic structure in guiding attention is exclusive to auditory context, which may explain

193 the findings from Experiment 1 that temporal structures generated by rhythmic changes

194 of auditory signals in the background automatically modulate the AB effect. To test this

195 idea, we designed Experiment 2 to directly investigate whether temporal structures based

196 on the change of visual properties would exert a similar influence on temporal attentional

197 deployment. In Experiment 2a, we used visual patterns with periodic change in

198 background color as the temporal context while observers were performing the same AB

199 task (Fig. 3A). As a control experiment, Experiment 2b followed the same logic for

200 Experiment 1b, in which we destroyed the structure of the visual context by changing the

201 background color in random orders, but kept the background color presented with the

202 targets the same as that in Experiment 2a (Fig. 3C).

203 Similar to findings obtained from Experiment 1a, the interaction between

204 experimental session (baseline vs. context session) and target position (between- vs.

205 within-cycle) was significant in Experiment 2a (Fig. 3B; $F(1, 15) = 5.180$, $p = .038$, η_p^2

206 $= .257$). In the context session only, T2 performance in the between-cycle condition was

207 better than that in the within-cycle condition ($t(15) = 3.538$, $p = .003$, Cohen's $d = 0.885$).

208 Compared with the baseline session, T2 performance was only improved in the between-

209 cycle condition ($t(15) = 2.274$, $p = .038$, Cohen's $d = 0.569$). By contrast, in Experiment 2b,

210 we did not observe a significant facilitation effect in the between-cycle condition

211 compared with the within-cycle condition ($t(15) = -1.176$, $p = .258$, Cohen's $d = 0.294$) or

212 with its counterpart in the baseline session ($t(15) = 0.685$, $p = .504$, Cohen's $d = 0.171$),

213 nor did we observe the interaction between experimental session and target position (Fig.

214 3D; $F(1, 15) = 1.435$, $p = .250$, $\eta_p^2 = .087$). These findings suggest that the utilization of

215 feature-based temporal regularities in attentional guidance is a fundamental principle

216 that holds true not only for auditory but also for visual processing.

217 **Excluding the impact of structure boundary: evidence from motion context**

218 So far, results from Experiments 1 and 2 have demonstrated a general regulatory effect

219 that feature-based temporal structure from task-irrelevant information recomposed

220 visual attentional allocation during the AB task, which could be exerted within the same

221 or cross different sensory modalities. In both experiments, however, the switch from one

222 feature-based rhythmic cycle to another was always accompanied by an abrupt change in

223 physical features (pitch or color), resulting in explicit boundaries before T2 presentation

224 in the between-cycle but not in the within-cycle condition. This abrupt change may serve

225 as an attentional cue or alerting signal for the upcoming T2, and thus accounts for the

226 improvement of performance in the between-cycle condition. To examine this possibility,

227 in Experiment 3, we introduced a cyclic motion context that possessed feature-based

228 rhythmicity identical to those contextual rhythms in previous experiments (for more

229 details, see Methods) but had no abrupt boundaries between cycles (Fig. 3E). Once again,

230   we observed significant improvement of T2 performance in the between-cycle condition

231   relative to the within-cycle condition in the cyclic motion session (Fig. 3F; $t(15) = 2.674$, p

232   $= .017$, Cohen's $d = 0.669$), but this was not the case in the random motion session ($t(15)$

233   $= -0.330$, $p = .746$, Cohen's $d = 0.082$), resulting in a significant interaction between

234   experimental session (baseline vs. context session) and target position (between- vs.

235   within-cycle): $F(1, 15) = 9.253$, $p = .008$, $\eta_p^2 = 0.382$. These results provide compelling

236   evidence that explicit perceptual boundaries are not necessary for the temporal structure

237   in the context to regulate the allocation of attentional resources.

238   **EEG experiment: The role of neural entrainment in regulating attentional**

239   **deployment**

240   *Neural tracking of higher-order temporal structure of contextual rhythms predicts the*

241   *behavioral modulation effect*

242   To investigate the neural mechanisms underlying the observed context-induced effect, we

243   carried out an EEG experiment using the same task as that in Experiment 1a. First of all,

244   we replicated the behavioral modulation effect that T2 performance was significantly

245   better in the between-cycle condition versus the within-cycle condition, only in the

246   context session (between-cycle: 0.567 ± 0.036, within-cycle: 0.520 ± 0.039, $t(15) = 3.838$,

247   $p = .002$, Cohen's $d = 0.960$) but not in the baseline session (between-cycle: 0.519 ± 0.039,

248   within-cycle: 0.527 ± 0.043, $t(15) = 0.296$, $p = .771$, Cohen's $d = 0.074$). Furthermore, to

249   identify the oscillatory characteristics of EEG signals in response to stimulus rhythms, we

250   examined the FFT spectral peaks by subtracting the mean power of two nearest

251   neighboring frequencies from the power at the stimulus frequency. Power spectrum in Fig.

252   4A shows several peaks for the context session, with the highest at 10 Hz (compared with

253   zero using one-sample t-test, right-tailed, $t(15) = 10.610$, $p < .001$, FDR-corrected for

254   multiple comparisons across frequencies) corresponding to the common stimulation

255   frequency of the visual and auditory streams. More importantly, the second-highest peak

256   appeared at 2.5 Hz ($t(15) = 5.730$, $p < .001$, FDR-corrected), followed by its harmonics at

257   5 and 7.5 Hz, indicating neural tracking of the feature-defined structure of the auditory

258   context. In contrast with the observation in the context session, we only found significant

10

power peak at 10 Hz (t(15) = 9.405, p < .001, FDR-corrected), but not at 2.5 Hz (t(15) = 0.301, p = .384, FDR-corrected) in the baseline session where contextual rhythms were absent, and the power at 2.5 Hz was significantly weaker than that in the context session (t(15) = 3.421, p = .002, FDR-corrected).

The significant enhancement of EEG power at 2.5 Hz clearly demonstrates that the brain can entrain to the higher-order structure defined by changes in an auditory feature (i.e. pitch) of the contextual stream. Consistent with previous studies, we also observed a wide range of individual variation in such cortical tracking of contextual rhythms (Grahn & McAuley, 2009; Kranczioch, 2017; Nozaradan et al., 2016). Could such variation predict one's ability to extract and utilize the feature-based structure at the neural level, and thus explain the individual differences in the attentional modulation effect? To explore this possibility, we calculated the Pearson correlation between the magnitude of the neural entrainment effect and the behavioral modulation index (BMI) using a cluster-based permutation test. In the context session, we identified two significant clusters showing positive correlation between power at 2.5 Hz and individuals' behavioral effect—one in the parieto-occipital region (Fig. 4B; P5, PO7, PO5, PO3; r =.587, p = .008, right-tailed) and the other in the frontal area (F3, F1, FZ, FC3, FC1, FCZ, C1, CZ; r =.681, p = .002). By contrast, no significant clusters were found in the baseline session (p > .05).

To further examine the role of brain activity phase-locked with the rhythmic context, we also analyzed the inter-trial phase coherence (ITPC) of EEG signals. Consistent with the power spectrum, ITPC in the context session peaked at 2.5 and 10 Hz (Fig. 4C), suggesting a hierarchical entrainment effect elicited by both feature-based and time-based regularities. By contrast, ITPC in the baseline session only peaked at 10 Hz, mirroring the stimulation rate of the visual stream, and the ITPC at 2.5 Hz was significantly weaker than that in the context session (t(15) = 4.652, p < .001, FDR corrected). Critically, only in the context session, the 2.5 Hz ITPC was positively correlated with the behavioral modulation index, yielding two significant clusters in the parieto-occipital area (Fig. 4D; P7, P5, PO7, PO5, PO3, O1: r = .612, p = .006) and the frontal area (FPZ, FP2, AF4, F2, F4, F6; r = .672, p = .002). Taken together, the results of power and ITPC jointly demonstrate that the better one's brain oscillations entrain to the higher-order temporal structure of

289   the contextual rhythms, the larger attentional enhancement one may exhibit in the

290   between-cycle condition over the within-cycle condition.

291   *T2-related alpha power reflects the attentional modulation*

292   Alpha oscillations have been considered to play a crucial and even causal role in temporal

293   attention, particularly in the AB effect (Hanslmayr et al., 2011; Klimesch, 2012). As the AB

294   phenomenon is characteristic of its stimulation frequency approximately at 10 Hz within

295   the alpha band, the brain can be in a resonant state with the AB stream at the same

296   frequency. It has been demonstrated that an increase in alpha power at the stimulus

297   frequency indicated attentional orienting to the stimulus stream, providing an on-line

298   measure of attentional allocation over the RSVP stream (Müller & Hübner, 2002). On the

299   other hand, enhanced alpha power in the AB task has also been shown to be associated

300   with correct T2 detection (Janson et al., 2014; Keil et al., 2006). Motivated by these

301   findings, we investigated whether alpha activity related to T2 processing could reflect the

302   attentional modulation in our study. We calculated alpha power around stimulation

303   frequency (9.5–10.5 Hz) within the time window of 0–100 ms after T2 onset, and found

304   two significant clusters for the context session—one in the left parieto-occipital region

305   (Fig. 5A; T7, C5, C3, TP7, CP5, CP3, P5, P3, PO5, PO3, O1) and the other in a right-lateralized

306   region (AF4, F2, F4, FC4, FC6, FT8, C4, C6, T8, CP4, CP6, TP8, P8), both showing stronger

307   alpha power in the between-cycle condition than in the within-cycle condition (for the left

308   cluster, $t(15) = 3.570$, $p = .0014$; for the right cluster, $t(15) = 3.631$, $p = .0012$, right-tailed,

309   cluster-based permutation test). This increase in T2-related alpha power, which could be

310   regarded as a sign of stimulus-driven neural activity, agrees well with the observations

311   that more attentional resources are deployed to T2 and thus higher accuracy was achieved

312   in the between-cycle condition than in the within-cycle condition.

313   *Cross-frequency coupling between delta phase and alpha power correlates with the*

314   *attentional modulation effect*

315   Examinations on delta-band entrainment effect and T2-related alpha power both reveal

316   behavioral relevance in our study. This leads to a natural question of whether the observed

12

317　attentional modulation effect is implemented through a coordinative process between

318　neural oscillations at delta and alpha bands. To address this question, we analyzed cross-

319　frequency coupling between delta phase and alpha power, which has been found to

320　support the attentional selection between competing stimuli (Gomez-Ramirez et al., 2011;

321　Wilson & Foxe, 2020; Wöstmann et al., 2016). We conducted the analysis in two clusters

322　whose neural responses in both the delta band (the ITPC at 2.5 Hz) and the alpha band

323　(T2-related alpha power) had an established link with the attentional modulation effect:

324　one in the parieto-occipital region (P5, PO3, PO5, O1) and the other in the frontal region

325　(AF4, F2, F4). We calculated the modulation index (MI) of phase-amplitude coupling (PAC)

326　between delta (1.5–3.5 Hz) and alpha band (7–13 Hz) for each cluster. The MI was

327　stronger in the between-cycle condition than in the within-cycle condition, while the

328　effect reached significance only in the parieto-occipital region (Fig. 5B; $t(15) = 2.432$, p

329　$= .028$) but not in the frontal region ($t(15) = 1.459$, $p = .165$). More importantly, this

330　contrast effect of delta-alpha PAC showed a positive correlation with the attentional

331　modulation effect on behavioral performance, which was also restricted to the parieto-

332　occipital region (Fig. 5C; $r = .660$, $p = .005$) and not found in the frontal region ($r = .154$, p

333　$= .569$). To further confirm the association between the delta-alpha PAC and the observed

334　attentional modulation effect, we did a cluster-based permutation test, which again

335　yielded a positively significant cluster in the parieto-occipital region (PO7, PO5, PO3, O1,

336　OZ; $r = .697$, $p = .003$). These results, combined with the findings from single-band

337　analyses, indicate that cortical tracking of hierarchical temporal structures of the auditory

338　context, as well as the coordination of such cortical tracking effects in delta and alpha

339　bands, may play a vital role in reconstructing the deployment of visual attentional in the

340　AB task.

Discussion

Temporal attention guided by time- and feature-based regularities

343　Dynamic information flows, such as speech and music, are composed of rhythmic

344　structures nested across multiple timescales (Ding et al., 2016; Gross et al., 2013; Koelsch

345　et al., 2013; Peelle & Davis, 2012). These hierarchical structures are organized in time

346 based on regularities in stimulus timing, that is, when sensory signals are emitted (time-
347 based), as well as regularities in information content, that is, how physical or semantic
348 features of the sensory inputs change over time (feature-based). Accrued evidence
349 suggests that temporal structures formed by time-based regularities are effective in
350 directing attention and enhance information selection at the expected time points (Jones
351 et al., 2002; Nobre et al., 2007; Nobre & van Ede, 2018). Yet the current study
352 demonstrates the role of feature-based temporal structures in recomposing temporal
353 attention deployment, which optimizes the distribution of attentional resources over two
354 temporally proximate targets in the AB task.

355 We modified the standard AB paradigm by introducing a contextual stream whose
356 physical property changed periodically to form perceivable, but unattended rhythmic
357 cycles in the background. Although this feature-based temporal structure was task-
358 irrelevant, it modulated the deployment of attentional resources along the AB stream, as
359 indicated by higher T2 detection performance when the two targets were located in
360 different cycles than in the same cycle. More intriguingly, this modulation effect was
361 observed no matter whether the contextual stream was from the auditory (Experiment 1)
362 or the visual (Experiment 2) modality. These findings provide clear evidence that
363 temporal structures defined by periodic changes of physical features in a dynamic context
364 can automatically reconstruct the temporal distribution of visual attention.

365 In the current study, the rhythmic cycles in the contextual stream consisted of a set of
366 temporally grouped items, some with abrupt changes in physical features across the cycle
367 boundaries. Could the attentional modulation effect be achieved purely on the basis of
368 transient perceptual boundaries or temporal grouping? Findings from several control
369 experiments do not agree with these assumptions. In Experiment 3, the rhythmic cycles
370 of contextual rhythms were defined by cyclic motion without any abrupt changes at the
371 boundaries. Even in this case, the cyclic motion yielded a significant attentional
372 modulation effect, excluding the possibility that the observed effect was caused simply by
373 perceptual changes of the background. In addition, results from Experiments 1d and 1e
374 further confirm that temporal attention guided by temporal regularities rather than
375 perceptual grouping is key to the reduced AB effect. On the one hand, simple grouping

376   without feature-based temporal regularities had little influence on T2 detection (as in

377   Experiment 1d, the feature-based grouping was irregular). On the other hand, when we

378   disrupted time-based regularities by using stochastic stimulus timing, the attentional

379   modulation effect also vanished, even though the rule of feature-based grouping remained

380   in force (as in Experiment 1e, every four identical tones constituted one group). Jointly,

381   these findings point to a mechanism of temporal attentional guidance independent of

382   transient perceptual cues and simple perceptual grouping.

383   It is worth noting that the attentional modulation effect did not occur in the absence

384   of regular stimulus timing. In other words, the feature-based regularities should work in

385   tandem with the time-based regularities to reconstruct the dynamics of visual temporal

386   attention, at least under the current experimental settings. This finding is consistent with

387   the emerging view concerning the role of a diversity of temporal structures in guiding

388   adaptive behavior (Nobre & van Ede, 2018). It has been suggested by studies using

389   auditory materials, mostly in speech and music perception, that temporal regularities

390   embedded in information content can act along with the time-based anticipation in

391   attentional guidance (Doelling & Poeppel, 2015; Morillon et al., 2016; Peelle & Davis, 2012;

392   Zion Golumbic et al., 2012). Our findings extend these studies by establishing a

393   mechanism in visual temporal attention that is guided by regularities in feature-defined

394   structures on top of the anticipation based on stimulation timing.

The roles of dynamic attentional deployment in reducing attentional blink and
boosting awareness

397   The AB phenomenon represents a bottleneck of conscious awareness pertaining to the

398   temporal resolution of visual attention. It is well known for its robustness that even long

399   repetitive training cannot eliminate the AB effect (Braun, 1998). Some studies have

400   demonstrated attenuated AB magnitude, as manifested in increased T2 detectability, by

401   enhancing T2 salience with color-salience training (Choi et al., 2012), emotional arousal

402   (Keil & Ihssen, 2004), or concurrent sounds (Olivers & Van der Burg, 2008). Another line

403   of research has also reported improved T2 performance when explicitly cueing the target-

404   onset-asynchrony (TOA) on a trial-by-trial basis (Martens & Johnson, 2005) or

405 manipulating the predictability of target onset (Tang et al., 2014; Visser et al., 2015).

406 Despite implementing different approaches, all these studies tried to manipulate certain

407 aspects of T2, regarding either its salience or predictability in time. By contrast, in our

408 study, the salience of targets and temporal expectations about T2 onset were comparable

409 across all experimental conditions. The only difference between the within- and between-

410 cycle conditions was the positions of the two targets relative to the feature-defined

411 temporal structure. Under this situation, items in the RSVP stream were no longer

412 encoded in isolation, but treated as a part of a structured information flow that could be

413 organized by periodic changes in the context. In particular, when T1 and T2 were

414 separated in different cycles, the temporal relations between them were reframed, which

415 might at least partially reduce the competition between the targets, thus improving the

416 resolution of visual temporal attentional and boosting the conscious access to T2. Instead

417 of emphasizing the role of a given target or a certain time point, our findings highlight the

418 significance of attentional deployment as a dynamic process in regulating visual

419 awareness and the AB effect, which is modulated by temporal structures of the entire

420 information flow.

421 **Neural entrainment to hierarchical contextual rhythms modulates dynamic**

422 **attending in visual perception**

423 Neural oscillations can be entrained to external rhythms across different frequencies

424 (Calderone et al., 2014; Escoffier et al., 2015; Henry et al., 2014; Mathewson et al., 2012;

425 Schroeder et al., 2010; Schroeder & Lakatos, 2009; Thut & Gross, 2011), allowing the brain

426 to encode dynamic information with multiplexed rhythmic structures across different

427 timescales (Fontolan et al., 2014; Lakatos et al., 2005; O'Connell et al., 2015). A common

428 example of this comes from studies of speech processing. The linguistic structure

429 possesses a temporal hierarchy—from smaller phonetic elements to larger syllabic and

430 phrasal units, which accordingly elicit neural entrainment at multiple frequency bands

431 (Arnal & Giraud, 2012; Zion Golumbic et al., 2012). There is growing evidence that cortical

432 tracking of the higher-order structures plays a vital role in speech and music

433 comprehension (Ding et al., 2016; Doelling & Poeppel, 2015; Gross et al., 2013; Koelsch et

434   al., 2013; Peelle & Davis, 2012). In our EEG study, we demonstrate an analogous

435   entrainment effect that not only keeps track of the original AB stream at 10 Hz but also

436   represents the higher-order feature-based structure of contextual rhythms at 2.5 Hz. More

437   importantly, the magnitude of the 2.5-Hz entrainment effect is significantly correlated

438   with the strength of the attentional modulation effect. The scalp topographic map of

439   correlation is lateralized and restricted to the left parietal region, which was found to be

440   associated with temporal attention (Bolger et al., 2014; Coull & Nobre, 1998). These

441   findings are in good accordance with the assumption that the cortical tracking of feature-

442   based contextual structure is critical to the redeployment of attentional resources over

443   the AB stream and may lead to the behavioral modulation effect.

444   The AB paradigm is characterized by its stimulation frequency approximately at 10

445   Hz within the alpha band. In our experiment, the 10-Hz power after T2 is stronger in the

446   between-cycle condition than in the within-cycle condition, which probably because the

447   increased attentional resources delivered to T2 enhance the stimulus-evoked neural

448   responses in the between-cycle condition (Janson et al., 2014; Keil et al., 2006). Further

449   analysis reveals that, in the left parieto-occipital cluster that exhibits phase-locked neural

450   responses to feature-based structures of the contextual rhythms and a T2-related

451   increment in alpha power, there is a phase-amplitude coupling between the delta and

452   alpha oscillations. Moreover, the strength of this delta-alpha coupling effect predicts the

453   effect of higher-order temporal structures on dynamic attentional allocation at the

454   individual level. These findings corroborate the idea that neural entrainment to a slower

455   external rhythm may serve as a mechanism of attentional selection, with the phase of delta

456   oscillation regulating the excitability of neural activity in the alpha band (Gomez-Ramirez

457   et al., 2011; Wilson & Foxe, 2020; Wöstmann et al., 2016).

458   Taken together, findings from the current study have cast new light on the classic

459   theory of DAT and its neural implementation. The DAT assumes attention to be inherently

460   oscillatory and can be driven by the timing pattern of external events (Jones, 1976; Jones

461   et al., 1982; Jones & Boltz, 1989; Large & Jones, 1999). By taking advantage of temporal

462   regularities of isochronous or rhythmic events, attentional synchrony can be established

463   and thus improve perceptual accuracy and elevate response speed. Our study extends the

464   DAT to more general cases of dynamic information processing at both the behavioral and

465   the neural levels. Primarily, our behavioral observations suggest that to utilize regularities

466   in a hierarchical temporal structure, the internal attentional oscillation may not only align

467   with first-order rhythmic structures based on stimulus timing, but also with higher-order

468   rhythmic structures defined by content-based changes of the information flow. Such a

469   dynamic attending process necessitates the synergy between time- and content-based

470   regularities, which could be implemented by neural entrainment to the higher-order

471   temporal structure and its coordination with the cortical tracking of the stimulus rhythm

472   through cross-frequency coupling.

473   **Conclusion**

474   In summary, the current study emphasizes the role of feature-defined contextual rhythms

475   in reconstructing the deployment of visual attention along dynamic information streams.

476   This work enriches our knowledge, as raised at the beginning of this article, about how

477   we optimize the limited mental capacity to process successive inputs from this ever-

478   changing world. Taking the AB phenomenon as an example, we provide a new perspective

479   on visual temporal attention research—when examining the perception of complex

480   dynamic information, temporal context on multiple timescales should be taken into

481   consideration because it provides a meaningful hierarchical temporal frame for

482   attentional deployment. This temporal frame, implemented by neural entrainment, may

483   serve to organize attentional resources in a prospective manner and help construct our

484   conscious experience of the world in the dimension of time.

Materials and Methods

Participants

A total of one hundred and forty-four volunteers (aged from 18 to 30 years, 69 females) were recruited and paid for their participation in the current study. One hundred and twenty-eight participated in the behavioral Experiments 1a-1e, 2a-2b, and 3 (16 for each experiment, with participants' gender balanced), and 16 (5 females) in the EEG experiment. All participants had normal or corrected-to-normal vision and normal hearing and were naïve to the purpose of the experiment. Considering the individual differences in the AB effect, only participants who exhibited a typical AB effect (i.e., an impairment of T2 accuracy at short lags compared with that at long lags) during a pre-screening session were asked to take part in the formal experiments. All participants provided written informed consent in accordance with experimental procedures and protocols approved by the Institutional Review Board of the Institute of Psychology, Chinese Academy of Sciences.

Stimuli

The rapid visual serial presentation (RSVP) stream used in the AB task consisted of 16 items (except in Experiments 1c and 1d). Among these items, one or two were the targets (capital letters selected from the alphabet, excluding B, D, O, I, M, Q, S, W, and Z), and the remaining were distractors (one-digit numbers, 1 and 0 excluded, without repetitions between any two of four successive digits). The items were displayed for 83 ms each and were separated by 17 ms blank intervals (except Experiment 1e), generating a 10 Hz rhythm based on stimulus presentation (see Fig. 1A, top). Each item subtended 0.47°×0.57° of visual angle and was displayed in white within a gray square (3°×3°) located at the center of a black screen. In each experiment, a contextual stream, which contained the same number of items as the AB stream but was organized by a feature-defined structure, was presented in synchronization with the AB stream. Stimuli were generated and displayed using MATLAB (The MathWorks Inc., Natick, MA) with the Psychophysics toolbox extension (Brainard, 1997). Visual stimuli were presented on a 21-inch CRT monitor with a viewing distance of 55 cm in a dim room. Auditory stimuli were delivered

514   binaurally over Bose QC3 headphones with the volume set to a comfortable listening level.

515   **Procedures**

516   **Behavioral Experiments**

517   In all experiments, participants were explicitly instructed to ignore the contextual events

518   and focused attention on the AB task. Participants initiated each trial by pressing the enter

519   key. A white fixation cross appeared for 600 ms at the center of the screen, followed by the

520   presentation of an AB stream (along with an auditory/visual stream in the context

521   session). After the last item disappeared, the central fixation turned blue to remind the

522   participant to report the identities of the target(s) in the order they detected them by

523   typing on the keyboard.

524   Experiment 1a had a baseline session followed by a context session. In the baseline

525   session, participants viewed only the AB stream and performed the typical AB task. To

526   induce the AB effect, the second target (T2) in the AB stream was located at the second

527   lag of the first target (T1) with a short stimulus onset asynchrony (SOA) of 200 ms, as the

528   magnitude of AB effect is most robust around the second and the third lags. In contrast

529   with the short-SOA condition, we introduced a long-SOA condition where T2 always

530   appeared at the 8th Lag of T1 and could rarely be missed. To measure the false alarm rate,

531   we also included catch trials in which only one target was displayed. The context session

532   had the same settings and task as the baseline session, except that a task-irrelevant

533   auditory stream was presented in synchronization with the original RSVP stream.

534   Specifically, the auditory stream was composed of 16 tones, each aligned with the onset of

535   a visual item and displayed for 30 ms. The tone sequence changed its pitch from high

536   (2000 Hz) to low (1200 Hz) or vice versa every four items (corresponding to 400 ms),

537   generating 4 auditory cycles (i.e., 4-4-4-4) at a rate of 2.5 Hz (Fig. 1A, middle). To examine

538   the regulation effect of such pitch-defined rhythmic structures, we created two

539   experimental conditions specifically for the short-SOA trials, by varying the positions of

540   T1 and T2 relative to the contextual cycles. In the "between-cycle condition", T1 and T2

541   were located in two adjacent cycles; and in the "within-cycle condition", the two targets

542   were located in the same cycle. To reduce observers' anticipation about the timing of T1

543 onset across trials, we introduced various T1 positions while keeping T2 located within

544 the middle two cycles. Each session had 120 experimental trials (40 trials for the between-

545 cycle, within-cycle, and long SOA condition each) and 20 catch trials. These trials were

546 divided into four equal blocks, with randomized trial order within each block.

547   Experiment 1b-1e adopted the same procedure as Experiment 1a but with the

548 following exceptions. In Experiment 1b, as shown in Fig. 1A (bottom), we abolished the

549 feature-based structure of the contextual streams by pseudo-randomizing the auditory

550 tone sequences while keeping the pitch of tones at target locations the same as that in

551 Experiment 1a. In Experiment 1c, we changed the temporal structure of the contextual

552 streams by altering their pitch change rate, generating two types of auditory sequences:

553 one with 4 five-tone cycles displayed at 2Hz (i.e., 5-5-5-5, see Fig. 2A, upper), and the other

554 with 5 three-tone cycles at 3.3 Hz (i.e., 3-3-3-3-3, see Fig. 2A, lower). For both frequency

555 conditions, T2 was located in the next to last or third from last cycles. In Experiment 1d,

556 we varied the length of chunks in the contextual streams, generating auditory sequences

557 with four cycles of different lengths (e.g., 5-2-4-3) but always having 4 tones in the third

558 cycle where the second target appeared (see Fig. 2C, upper). In Experiment 1e, the feature-

559 based structure remained while the rhythm from stimulus timing was removed (see Fig.

560 2C, lower). Specifically, the tone pitch changed every four items just as in Experiment 1a,

561 whereas the stimulus onset asynchrony (SOA) of each visual item was selected randomly

562 from a predetermined uniform distribution (50, 67, 83, 100, 100, 117, 133, 150 ms) to

563 keep the total presentation time identical to that in Experiment 1a. In both Experiment 1d

564 and 1e, T2 was always the second item in the 3rd cycle for the between-cycle condition

565 and the last item in the 3rd cycle for the within-cycle condition.

566   Experiments 2a and 2b had a design similar to that of Experiments 1a and 1b, except

567 that we replaced the auditory context with a visually presented contextual stream that

568 possessed color-defined temporal structure. Specifically, in the context session of

569 Experiment 2a, the color of the background square changed from green to red or vice

570 versa at the same tempo as that for contextual tones in Experiment 1a (Fig. 3A, upper).

571 And in Experiment 2b, the background color changed in arrhythmic patterns (Fig. 3C,

572 upper). Luminance of the two colors was matched for each observer with a chromatic

21

573   flicker fusion procedure before the experiments.

574   Experiment 3 consisted of an experimental session with a structured context as that

575   in Experiment 2a and a control session with a random context as that in Experiment 2b.

576   In the experimental session, the contextual rhythm was created by cyclic motion patterns

577   in the background (Fig. 3E, upper). Specifically, a blue right-angle (width = 0.38°, side

578   length = 1.5°), initiating from one corner (the upper-left or the upper-right, balanced

579   between blocks) of the background square, rotated clockwise at the same pace as the AB

580   stream. In this way, one cycle of rotation corresponded to the appearance of four items

581   (i.e., 400 ms), forming a 2.5 Hz structure based on the motion cycles. In the control session,

582   no cyclic motion pattern remained but the right-angle shifted to a random quadrant under

583   the constraint of identical initial quadrant in each 'cycle' (Fig. 3E, lower).

584   Note that in all these experiments, we also labelled the conditions in baseline and

585   control sessions as "within-cycle" or "between-cycle", just to indicate that these conditions

586   shared the same absolute target positions with the corresponding conditions in the

587   context session. This design was adopted to control for any potential influence of the

588   absolute position of a target within the AB stream. Specifically, for each experimental

589   condition (within- or between-cycle), we matched the absolute positions of T1 and T2

590   between the context session and the baseline session without a context (Experiments 1–

591   2), or between the experimental session and the control session with a random context

592   (Experiments 1 & 3).

593   **EEG Experiment**

594   The procedure of the EEG experiment was mostly identical to that of Experiment 1a except

595   for the following modifications. Black items were presented on a gray background and the

596   item size was 0.59°×0.78°. In each trial, the fixation duration was 1000 ms and each item

597   was displayed for 100 ms with no blank interval. After response, there was a 1.2–1.5 s

598   blank interval. Each subject completed 3 baseline blocks followed by 6 experimental

599   blocks with the auditory context. Each block consisted of 40 trials, with 17 short-SOA trials

600   in each of the between- and within-cycle condition, and the remaining 6 as the catch trials,

601   run in a random order.

EEG recording

602

603 A SynAmps[2] Neuroscan amplifier system (Compumedics Ltd, Abbotsford, Australia) was

604 used for data acquisition. EEG signals were recorded continuously from 64 Ag/AgCl

605 electrodes mounted on an elastic cap according to the extended 10–20 system, with a

606 reference electrode placed between Cz and CPz. Vertical and horizontal eye movements

607 were monitored with two bipolar EOG electrode pairs positioned above and below the left

608 eye and on the outer canthus of each eye. Data were acquired at a sampling rate of 1000

609 Hz with an online 0.05-100 Hz band-pass filter (notched at 50 Hz). Electrode impedances

610 were kept below 8 kΩ for all electrodes.

EEG data analysis

611

612 *Preprocessing*

613 Data preprocessing and analysis was performed using EEGLAB toolbox (Delorme &

614 Makeig, 2004) and FieldTrip (Oostenveld et al., 2011) in combination with custom

615 MATLAB scripts. EEG recordings were down-sampled offline to 500 Hz, high-pass filtered

616 at 0.3 Hz, and then segmented into 2200 ms trials from -600 to 1600 ms relative to the

617 onset of the AB stream. Ocular artifacts were then identified and removed using the

618 ADJUST algorithm (Mognon et al., 2011) based on independent component analysis (ICA).

619 Segments with voltage deflections greater than 75 uV were rejected. Residual artifacts

620 were checked by visual inspection. On average, 90 trials remained for each condition and

621 each individual. The segmented data were re-referenced to the average potential of all

622 electrodes excluding the mastoid and EOG electrodes.

623 *Power analysis*

624 The preprocessed EEG signals were first corrected by subtracting the average activity of

625 the entire stream for each epoch, and then averaged across trials for each condition, each

626 participant, and each electrode. Then signals from stream onset were zero-padded and

627 fast Fourier transformed, yielding amplitude and phase estimation at a frequency

628 resolution of 0.5 Hz. Power spectra was calculated as the squared amplitude and then

629 converted to decibel scale (i.e., $10*\log_{10}$). To remove unrelated background noises from

23

630   the frequency response of stimulus rhythms, for each frequency, the mean power at two

631   nearest neighboring frequencies was subtracted from the power at that center frequency.

632   The subtracted power at each frequency was then averaged across all channels (excluding

633   M1, M2, VEO, HEO, CB1 and CB2) and compared with zero using one-sample t test to

634   determine whether neural oscillations were entrained to temporal structures of the

635   stimulus rhythms. Multiple comparisons across frequencies were controlled by the false

636   discovery rate (FDR, $p < .05$) procedure.

637   *Phase locking analysis*

638   Inter-trial phase coherence (ITPC) serves to indicate the consistency with which intrinsic

639   neural oscillations were phase-locked to the external rhythms over trials. We first

640   obtained phase estimation from spectral decomposition for each single trial based on fast

641   Fourier transform, and then calculated ITPC as follows:

642    $$\text{ITPC}(f) = \left| \frac{1}{n} \sum_{k=1}^{n} \left(\frac{F_k(f)}{|F_k(f)|} \right) \right| \qquad (1)$$

643   where, for n trials, $F_k(f)$ is the spectral estimate of trial k at frequency f, and $||$ represents

644   the complex norm.

645   *T2-related alpha power*

646   In order to measure the neural activity time-locked to T2 at alpha band, time-frequency

647   analysis was performed by convolving single-trial data with a complex Morlet tapered

648   wavelet using the *newtimef* function of EEGLAB. To optimize the trade-off between

649   temporal and frequency resolution, the length of wavelets increased linearly from 1 cycle

650   at the lowest frequency (2 Hz) to 7.5 cycles at the highest frequency (30 Hz, in increments

651   of 0.5 Hz), resulting in power estimates from -321 to 1321 ms around stream onset. For

652   each frequency, power at each time point was first averaged across trials and then divided

653   by the average activity in baseline period from -300 to -200 ms and log-transformed to

654   decibels.

655

656 *Delta-alpha phase-amplitude coupling analysis*

657 The modulation index (MI) of phase-amplitude coupling (PAC) was used to measure the

658 coordinative modulation between the phase of ongoing oscillations in delta band (1.5–3.5

659 Hz) and the power in alpha bands (7–13 Hz) at each electrode. First, the low-frequency

660 phase at delta band (f_p) and high-frequency amplitude at alpha band (f_a) were estimated

661 by filtering each epoch with a Butterworth bandpass filter and then applying the Hilbert

662 transform. The broad bandwidth of alpha band (7–13 Hz) was determined to be wide

663 enough to contain the side-bands of the modulating frequency at f_p (2.5 Hz) (Dvorak &

664 Fenton, 2014; Seymour et al., 2017). Next, the modulation index of PAC was quantified

665 using the mean-vector length method first introduced by Canolty et al. (Canolty et al.,

666 2006). As shown in formula (2), for each epoch, the MI values were calculated by

667 combining low-frequency phase and high-frequency amplitude into complex time series

668 and then taking the length of the average vector within the selected time window (500–

669 1300 ms relative to stream onset), which corresponded to the middle two cycles of the

670 contextual stream. The first and last 400 ms of the stream was discarded to avoid the edge

671 artifacts after bandpass filtering. The resulting MI values were then averaged across trials

672 for each condition.

673 $\text{MI} = \left| \frac{1}{N} \sum_{n=1}^{N} A_H(n) e^{i(\Phi_L(n))} \right|$ (2)

674 where MI is estimated for a single trial with length of N samples or time points, $A_H(n)$ is

675 the amplitude of higher-frequency at time point n, $\Phi_L(n)$ is the phase of lower-frequency

676 at time point n, and || represents the complex norm.

677 *Correlation analysis*

678 To examine whether the above EEG indices were associated with the observed attentional

679 modulation effect, we correlated these EEG indices with individual's behavioral

680 modulation index (BMI), which was determined by the following formula:

681 $\text{BMI} = \frac{P_{BET} - P_{WIT}}{P_{BET} + P_{WIT}}$ (3)

682   where P_{BET} and P_{WIT} were the accuracy rate of T2 identification in the between-cycle

683   and the within-cycle conditions in the context session, respectively.

684   *Cluster-based permutation test*

685   To identify clusters of channels that are significant in each statistical test, we used the

686   cluster-based permutation test, which was first stated by Maris and Oostenveld (Maris &

687   Oostenveld, 2007) and used in a number of previous studies (Doelling & Poeppel, 2015;

688   Spaak et al., 2014). Firstly, cluster-level statistics are calculated as the sum of channel-

689   specific test statistics within every cluster. Then, the maximum of the cluster-level

690   statistics is taken as the actual test statistic. Finally, the significance probability of the

691   maximum cluster-level statistic is evaluated under the permutation distribution obtained

692   with the Monte Carlo method in which the permutation cluster-level statistic is calculated

693   by randomly swapping the conditions in participants 1000 times.

26

Acknowledgements

Competing interests

701 The authors declare that no competing interests exist.

References

Arnal, L. H., & Giraud, A.-L. (2012). Cortical oscillations and sensory predictions. *Trends in Cognitive Sciences*, *16*(7), 390–398. https://doi.org/10.1016/j.tics.2012.05.003

Bolger, D., Coull, J. T., & Schön, D. (2014). Metrical Rhythm Implicitly Orients Attention in Time as Indexed by Improved Target Detection and Left Inferior Parietal Activation. *Journal of Cognitive Neuroscience*, *26*(3), 593–605. https://doi.org/10.1162/jocn_a_00511

Brainard, D. H. (1997). The Psychophysics Toolbox. *Spatial Vision*, *10*(4), 433–436. https://doi.org/10.1163/156856897X00357

Braun, J. (1998). Vision and attention: The role of training. *Nature*, *393*(6684), 424–425. https://doi.org/10.1038/30875

Bregman, A. S. (1994). *Auditory Scene Analysis: The Perceptual Organization of Sound*. MIT Press.

Broadbent, D. E., & Broadbent, M. H. P. (1987). From detection to identification: Response to multiple targets in rapid serial visual presentation. *Perception & Psychophysics*, *42*(2), 105–113. https://doi.org/10.3758/BF03210498

Brochard, R., Tassin, M., & Zagar, D. (2013). Got rhythm… for better and for worse. Cross-modal effects of auditory rhythm on visual word recognition. *Cognition*, *127*(2), 214–219. https://doi.org/10.1016/j.cognition.2013.01.007

Calderone, D. J., Lakatos, P., Butler, P. D., & Castellanos, F. X. (2014). Entrainment of neural oscillations as a modifiable substrate of attention. *Trends in Cognitive Sciences*, *18*(6), 300–309. https://doi.org/10.1016/j.tics.2014.02.005

Canolty, R. T., Edwards, E., Dalal, S. S., Soltani, M., Nagarajan, S. S., Kirsch, H. E., Berger, M. S., Barbaro, N. M., & Knight, R. T. (2006). High Gamma Power Is Phase-Locked to Theta Oscillations in Human Neocortex. *Science*, *313*(5793), 1626–1628. https://doi.org/10.1126/science.1128115

Choi, H., Chang, L.-H., Shibata, K., Sasaki, Y., & Watanabe, T. (2012). Resetting capacity limitations revealed by long-lasting elimination of attentional blink through training. *Proceedings of the National Academy of Sciences*, *109*(30), 12242–12247. https://doi.org/10.1073/pnas.1203972109

Chun, M. M., & Potter, M. C. (1995). A two-stage model for multiple target detection in rapid serial visual presentation. *Journal of Experimental Psychology: Human Perception and Performance*, *21*(1), 109–127. https://doi.org/10.1037/0096-1523.21.1.109

Coull, J. T., & Nobre, A. C. (1998). Where and When to Pay Attention: The Neural Systems for Directing Attention to Spatial Locations and to Time Intervals as Revealed by Both PET and fMRI. *The Journal of Neuroscience*, *18*(18), 7426–7435. https://doi.org/10.1523/JNEUROSCI.18-18-07426.1998

Delorme, A., & Makeig, S. (2004). EEGLAB: An open source toolbox for analysis of single-trial EEG dynamics including independent component analysis. *Journal of Neuroscience Methods*, *134*(1), 9–21. https://doi.org/10.1016/j.jneumeth.2003.10.009

Ding, N., Melloni, L., Zhang, H., Tian, X., & Poeppel, D. (2016). Cortical tracking of

745   hierarchical linguistic structures in connected speech. *Nature Neuroscience*, *19*(1),
746   158–164. https://doi.org/10.1038/nn.4186

747 Doelling, K. B., & Poeppel, D. (2015). Cortical entrainment to music and its modulation by
748   expertise. *Proceedings of the National Academy of Sciences*, 201508431.
749   https://doi.org/10.1073/pnas.1508431112

750 Dux, P. E., & Marois, R. (2009). The attentional blink: A review of data and theory.
751   *Attention, Perception, & Psychophysics*, *71*(8), 1683–1700.
752   https://doi.org/10.3758/APP.71.8.1683

753 Dvorak, D., & Fenton, A. A. (2014). Toward a proper estimation of phase–amplitude
754   coupling in neural oscillations. *Journal of Neuroscience Methods*, *225*, 42–56.
755   https://doi.org/10.1016/j.jneumeth.2014.01.002

756 Escoffier, N., Herrmann, C. S., & Schirmer, A. (2015). Auditory rhythms entrain visual
757   processes in the human brain: Evidence from evoked oscillations and event-related
758   potentials. *NeuroImage*, *111*, 267–276.
759   https://doi.org/10.1016/j.neuroimage.2015.02.024

760 Fontolan, L., Morillon, B., Liegeois-Chauvel, C., & Giraud, A.-L. (2014). The contribution of
761   frequency-specific activity to hierarchical information processing in the human
762   auditory cortex. *Nature Communications*, *5*, 4694.
763   https://doi.org/10.1038/ncomms5694

764 Gomez-Ramirez, M., Kelly, S. P., Molholm, S., Sehatpour, P., Schwartz, T. H., & Foxe, J. J.
765   (2011). Oscillatory Sensory Selection Mechanisms during Intersensory Attention to
766   Rhythmic Auditory and Visual Inputs: A Human Electrocorticographic Investigation.
767   *The Journal of Neuroscience*, *31*(50), 18556–18567.
768   https://doi.org/10.1523/JNEUROSCI.2164-11.2011

769 Grahn, J. A., & McAuley, J. D. (2009). Neural bases of individual differences in beat
770   perception. *NeuroImage*, *47*(4), 1894–1903.
771   https://doi.org/10.1016/j.neuroimage.2009.04.039

772 Gross, J., Hoogenboom, N., Thut, G., Schyns, P., Panzeri, S., Belin, P., & Garrod, S. (2013).
773   Speech Rhythms and Multiplexed Oscillatory Sensory Coding in the Human Brain.
774   *PLoS Biol*, *11*(12). https://doi.org/10.1371/journal.pbio.1001752

775 Haegens, S., & Zion Golumbic, E. (2018). Rhythmic facilitation of sensory processing: A
776   critical review. *Neuroscience & Biobehavioral Reviews*, *86*, 150–165.
777   https://doi.org/10.1016/j.neubiorev.2017.12.002

778 Hanslmayr, S., Gross, J., Klimesch, W., & Shapiro, K. L. (2011). The role of alpha
779   oscillations in temporal attention. *Brain Research Reviews*, *67*(1–2), 331–343.
780   https://doi.org/10.1016/j.brainresrev.2011.04.002

781 Henry, M. J., & Herrmann, B. (2014). Low-frequency neural oscillations support dynamic
782   attending in temporal context. *Timing & Time Perception*, *2*, 62–86.
783   https://doi.org/10.1163/22134468-00002011

784 Henry, M. J., Herrmann, B., & Obleser, J. (2014). Entrained neural oscillations in multiple
785   frequency bands comodulate behavior. *Proceedings of the National Academy of
786   Sciences*, *111*(41), 14935–14940. https://doi.org/10.1073/pnas.1408741111

787 Janson, J., De Vos, M., Thorne, J. D., & Kranczioch, C. (2014). Endogenous and Rapid Serial
788   Visual Presentation-induced Alpha Band Oscillations in the Attentional Blink.

789   *Journal of Cognitive Neuroscience*, *26*(7), 1454–1468.

790   https://doi.org/10.1162/jocn_a_00551

791 Jones, M. R. (1976). Time, our lost dimension: Toward a new theory of perception,

792   attention, and memory. *Psychological Review*, *83*(5), 323–355.

793   https://doi.org/10.1037/0033-295X.83.5.323

794 Jones, M. R., & Boltz, M. (1989). Dynamic attending and responses to time. *Psychological*

795   *Review*, *96*(3), 459–491. https://doi.org/10.1037/0033-295X.96.3.459

796 Jones, M. R., Boltz, M., & Kidd, G. (1982). Controlled attending as a function of melodic

797   and temporal context. *Perception & Psychophysics*, *32*(3), 211–218.

798   https://doi.org/10.3758/BF03206225

799 Jones, M. R., Kidd, G., & Wetzel, R. (1981). Evidence for rhythmic attention. *Journal of*

800   *Experimental Psychology: Human Perception and Performance*, *7*(5), 1059–1073.

801   https://doi.org/10.1037/0096-1523.7.5.1059

802 Jones, M. R., Moynihan, H., MacKenzie, N., & Puente, J. (2002). Temporal Aspects of

803   Stimulus-Driven Attending in Dynamic Arrays. *Psychological Science*, *13*(4), 313–

804   319. https://doi.org/10.1111/1467-9280.00458

805 Keil, A., & Ihssen, N. (2004). Identification Facilitation for Emotionally Arousing Verbs

806   During the Attentional Blink. *Emotion*, *4*(1), 23–35. https://doi.org/10.1037/1528-

807   3542.4.1.23

808 Keil, A., Ihssen, N., & Heim, S. (2006). Early cortical facilitation for emotionally arousing

809   targets during the attentional blink. *BMC Biology*, *4*(1), 23.

810   https://doi.org/10.1186/1741-7007-4-23

811 Klimesch, W. (2012). Alpha-band oscillations, attention, and controlled access to stored

812   information. *Trends in Cognitive Sciences*, *16*(12), 606–617.

813   https://doi.org/10.1016/j.tics.2012.10.007

814 Koelsch, S., Rohrmeier, M., Torrecuso, R., & Jentschke, S. (2013). Processing of

815   hierarchical syntactic structure in music. *Proceedings of the National Academy of*

816   *Sciences*, *110*(38), 15443–15448. https://doi.org/10.1073/pnas.1300272110

817 Kranczioch, C. (2017). Individual differences in dual-target RSVP task performance

818   relate to entrainment but not to individual alpha frequency. *PLOS ONE*, *12*(6),

819   e0178934. https://doi.org/10.1371/journal.pone.0178934

820 Lakatos, P., Karmos, G., Mehta, A. D., Ulbert, I., & Schroeder, C. E. (2008). Entrainment of

821   Neuronal Oscillations as a Mechanism of Attentional Selection. *Science*, *320*(5872),

822   110–113. https://doi.org/10.1126/science.1154735

823 Lakatos, P., Musacchia, G., O'Connel, M. N., Falchier, A. Y., Javitt, D. C., & Schroeder, C. E.

824   (2013). The Spectrotemporal Filter Mechanism of Auditory Selective Attention.

825   *Neuron*, *77*(4), 750–761. https://doi.org/10.1016/j.neuron.2012.11.034

826 Lakatos, P., Shah, A. S., Knuth, K. H., Ulbert, I., Karmos, G., & Schroeder, C. E. (2005). An

827   Oscillatory Hierarchy Controlling Neuronal Excitability and Stimulus Processing in

828   the Auditory Cortex. *Journal of Neurophysiology*, *94*(3), 1904–1911.

829   https://doi.org/10.1152/jn.00263.2005

830 Large, E. W., & Jones, M. R. (1999). The dynamics of attending: How people track time-

831   varying events. *Psychological Review*, *106*(1), 119. https://doi.org/10.1037/0033-

832   295X.106.1.119

833   Maris, E., & Oostenveld, R. (2007). Nonparametric statistical testing of EEG- and MEG-
834   data. *Journal of Neuroscience Methods*, *164*(1), 177–190.
835   https://doi.org/10.1016/j.jneumeth.2007.03.024

836   Martens, S., & Johnson, A. (2005). Timing attention: Cuing target onset interval
837   attenuates the attentional blink. *Memory & Cognition*, *33*(2), 234–240.
838   https://doi.org/10.3758/BF03195312

839   Martens, S., & Wyble, B. (2010). The attentional blink: Past, present, and future of a blind
840   spot in perceptual awareness. *Neuroscience & Biobehavioral Reviews*, *34*(6), 947–
841   957. https://doi.org/10.1016/j.neubiorev.2009.12.005

842   Mathewson, K. E., Fabiani, M., Gratton, G., Beck, D. M., & Lleras, A. (2010). Rescuing
843   stimuli from invisibility: Inducing a momentary release from visual masking with
844   pre-target entrainment. *Cognition*, *115*(1), 186–191.
845   https://doi.org/10.1016/j.cognition.2009.11.010

846   Mathewson, K. E., Prudhomme, C., Fabiani, M., Beck, D. M., Lleras, A., & Gratton, G. (2012).
847   Making Waves in the Stream of Consciousness: Entraining Oscillations in EEG Alpha
848   and Fluctuations in Visual Awareness with Rhythmic Visual Stimulation. *Journal of*
849   *Cognitive Neuroscience*, *24*(12), 2321–2333. https://doi.org/10.1162/jocn_a_00288

850   Miller, J. E., Carlson, L. A., & McAuley, J. D. (2013). When What You Hear Influences When
851   You See Listening to an Auditory Rhythm Influences the Temporal Allocation of
852   Visual Attention. *Psychological Science*, *24*(1), 11–18.
853   https://doi.org/10.1177/0956797612446707

854   Mognon, A., Jovicich, J., Bruzzone, L., & Buiatti, M. (2011). ADJUST: An automatic EEG
855   artifact detector based on the joint use of spatial and temporal features.
856   *Psychophysiology*, *48*(2), 229–240. https://doi.org/10.1111/j.1469-
857   8986.2010.01061.x

858   Morillon, B., Schroeder, C. E., Wyart, V., & Arnal, L. H. (2016). Temporal Prediction in lieu
859   of Periodic Stimulation. *Journal of Neuroscience*, *36*(8), 2342–2347.
860   https://doi.org/10.1523/JNEUROSCI.0836-15.2016

861   Müller, M. M., & Hübner, R. (2002). Can the Spotlight of Attention Be Shaped Like a
862   Doughnut? Evidence From Steady-State Visual Evoked Potentials. *Psychological*
863   *Science*, *13*(2), 119–124. https://doi.org/10.1111/1467-9280.00422

864   Nobre, A. C., Correa, A., & Coull, J. (2007). The hazards of time. *Current Opinion in*
865   *Neurobiology*, *17*(4), 465–470. https://doi.org/10.1016/j.conb.2007.07.006

866   Nobre, A. C., & van Ede, F. (2018). Anticipated moments: Temporal structure in attention.
867   *Nature Reviews Neuroscience*, *19*(1), 34–48. https://doi.org/10.1038/nrn.2017.141

868   Nozaradan, S., Peretz, I., & Keller, P. E. (2016). Individual Differences in Rhythmic Cortical
869   Entrainment Correlate with Predictive Behavior in Sensorimotor Synchronization.
870   *Scientific Reports*, *6*, 20612. https://doi.org/10.1038/srep20612

871   Obleser, J., & Kayser, C. (2019). Neural Entrainment and Attentional Selection in the
872   Listening Brain. *Trends in Cognitive Sciences*, *23*(11), 913–926.
873   https://doi.org/10.1016/j.tics.2019.08.004

874   O'Connell, M. N., Barczak, A., Ross, D., McGinnis, T., Schroeder, C. E., & Lakatos, P. (2015).
875   Multi-Scale Entrainment of Coupled Neuronal Oscillations in Primary Auditory
876   Cortex. *Frontiers in Human Neuroscience*, 655.

877   https://doi.org/10.3389/fnhum.2015.00655

878   Olivers, C. N. L., & Van der Burg, E. (2008). Bleeping you out of the blink: Sound saves
879   vision from oblivion. *Brain Research*, *1242*, 191–199.
880   https://doi.org/10.1016/j.brainres.2008.01.070

881   Oostenveld, R., Fries, P., Maris, E., & Schoffelen, J.-M. (2011). FieldTrip: Open Source
882   Software for Advanced Analysis of MEG, EEG, and Invasive Electrophysiological
883   Data. *Computational Intelligence and Neuroscience*, *2011*, e156869.
884   https://doi.org/10.1155/2011/156869

885   Peelle, J. E., & Davis, M. H. (2012). Neural oscillations carry speech rhythm through to
886   comprehension. *Frontiers in Psychology*, *3*, 320.
887   https://doi.org/10.3389/fpsyg.2012.00320

888   Posner, M. I. (1980). Orienting of attention. *Quarterly Journal of Experimental Psychology*,
889   *32*(1), 3–25. https://doi.org/10.1080/00335558008248231

890   Raymond, J. E., Shapiro, K. L., & Arnell, K. M. (1992). Temporary suppression of visual
891   processing in an RSVP task: An attentional blink? *Journal of Experimental*
892   *Psychology: Human Perception and Performance*, *18*(3), 849–860.
893   https://doi.org/10.1037/0096-1523.18.3.849

894   Schroeder, C. E., & Lakatos, P. (2009). Low-frequency neuronal oscillations as
895   instruments of sensory selection. *Trends in Neurosciences*, *32*(1), 9–18.
896   https://doi.org/10.1016/j.tins.2008.09.012

897   Schroeder, C. E., Wilson, D. A., Radman, T., Scharfman, H., & Lakatos, P. (2010). Dynamics
898   of Active Sensing and perceptual selection. *Current Opinion in Neurobiology*, *20*(2),
899   172–176. https://doi.org/10.1016/j.conb.2010.02.010

900   Seymour, R. A., Rippon, G., & Kessler, K. (2017). The Detection of Phase Amplitude
901   Coupling during Sensory Processing. *Frontiers in Neuroscience*, *11*.
902   https://doi.org/10.3389/fnins.2017.00487

903   Shapiro, K. L., Raymond, J. E., & Arnell, K. M. (1997). The attentional blink. *Trends in*
904   *Cognitive Sciences*, *1*(8), 291–296. https://doi.org/10.1016/S1364-6613(97)01094-
905   2

906   Spaak, E., Lange, F. P. de, & Jensen, O. (2014). Local Entrainment of Alpha Oscillations by
907   Visual Stimuli Causes Cyclic Modulation of Perception. *The Journal of Neuroscience*,
908   *34*(10), 3536–3544. https://doi.org/10.1523/JNEUROSCI.4385-13.2014

909   Tang, M. F., Badcock, D. R., & Visser, T. A. W. (2014). Training and the attentional blink:
910   Limits overcome or expectations raised? *Psychonomic Bulletin & Review*, *21*(2), 406–
911   411. https://doi.org/10.3758/s13423-013-0491-3

912   ten Oever, S., Schroeder, C. E., Poeppel, D., van Atteveldt, N., & Zion-Golumbic, E. (2014).
913   Rhythmicity and cross-modal temporal cues facilitate detection. *Neuropsychologia*,
914   *63*, 43–50. https://doi.org/10.1016/j.neuropsychologia.2014.08.008

915   Thut, G., & Gross, J. (2011). Entrainment of perceptually relevant brain oscillations by
916   non-invasive rhythmic stimulation of the human brain. *Frontiers in Perception*
917   *Science*, *2*, 170. https://doi.org/10.3389/fpsyg.2011.00170

918   Visser, T. A. W., Ohan, J. L., & Enns, J. T. (2015). Temporal cues derived from statistical
919   patterns can overcome resource limitations in the attentional blink. *Attention,*
920   *Perception, & Psychophysics*, *77*(5), 1585–1595. https://doi.org/10.3758/s13414-

921   015-0880-y

922   Wilson, T. J., & Foxe, J. J. (2020). Cross-frequency coupling of alpha oscillatory power to

923   the entrainment rhythm of a spatially attended input stream. *Cognitive*

924   *Neuroscience*, *11*(1–2), 71–91. https://doi.org/10.1080/17588928.2019.1627303

925   Wöstmann, M., Herrmann, B., Maess, B., & Obleser, J. (2016). Spatiotemporal dynamics of

926   auditory attention synchronize with speech. *Proceedings of the National Academy of*

927   *Sciences*, *113*(14), 3873–3878. https://doi.org/10.1073/pnas.1523357113

928   Zion Golumbic, E. M., Poeppel, D., & Schroeder, C. E. (2012). Temporal context in speech

929   processing and attentional stream selection: A behavioral and neural perspective.

930   *Brain and Language*, *122*(3), 151–161.

931   https://doi.org/10.1016/j.bandl.2011.12.010

932

933

Figures

Figure 1
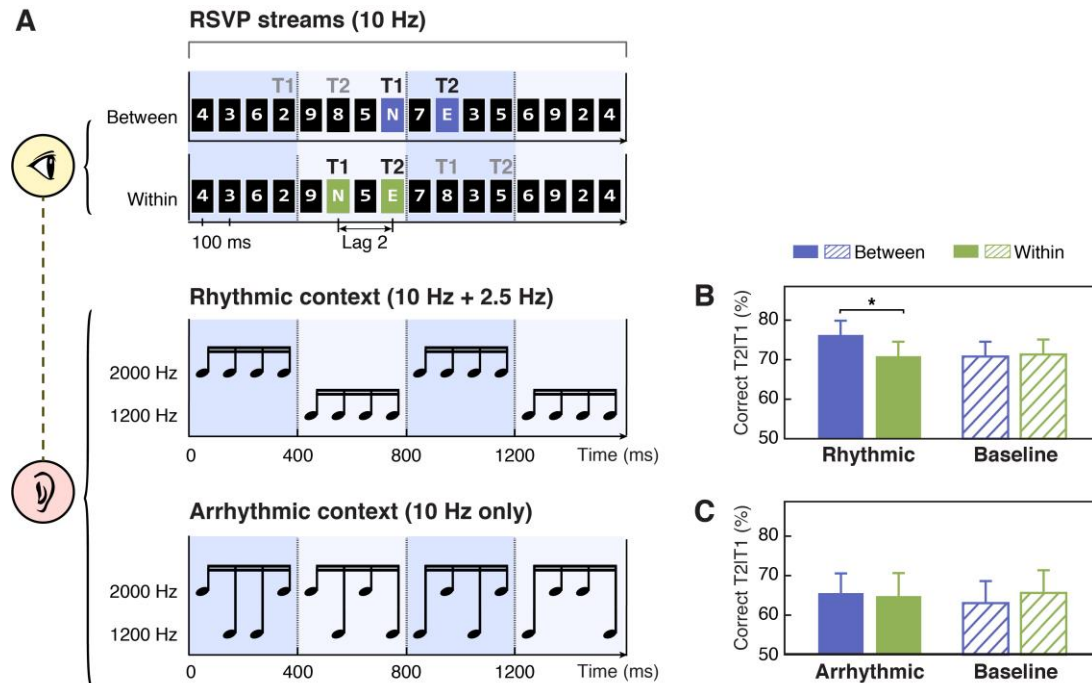

Fig. 1. Schematics of stimuli and results for Experiments 1a and 1b. (A) In the AB task, participants were presented with rapid serial visual presentation (RSVP) streams at 10 Hz (top). Each stream contained two capital letter targets embedded in fourteen number distractors. Black and gray "T1" and "T2" denote two alternative options for target locations in the short-SOA conditions. These targets were located either in two adjacent cycles (the between-cycle condition, displayed on violet background for illustration only) or within the same rhythmic cycle (the within-cycle condition, displayed on green background for illustration only) defined by a rhythmic auditory context in Experiment 1a (middle). Arrhythmic context was used as a control in Experiment 1b (bottom). (B & C) T2 detection accuracy conditioned on correct T1 response for the experiments using rhythmic and arrhythmic contexts. Note that in the baseline (visual-only) session, the labels of "between" and "within" were used to refer to the conditions where the two targets shared the same absolute positions with their corresponding conditions in the context (audiovisual) session. Error bars represent 1 SEM; * $p<0.05$.

Figure 2
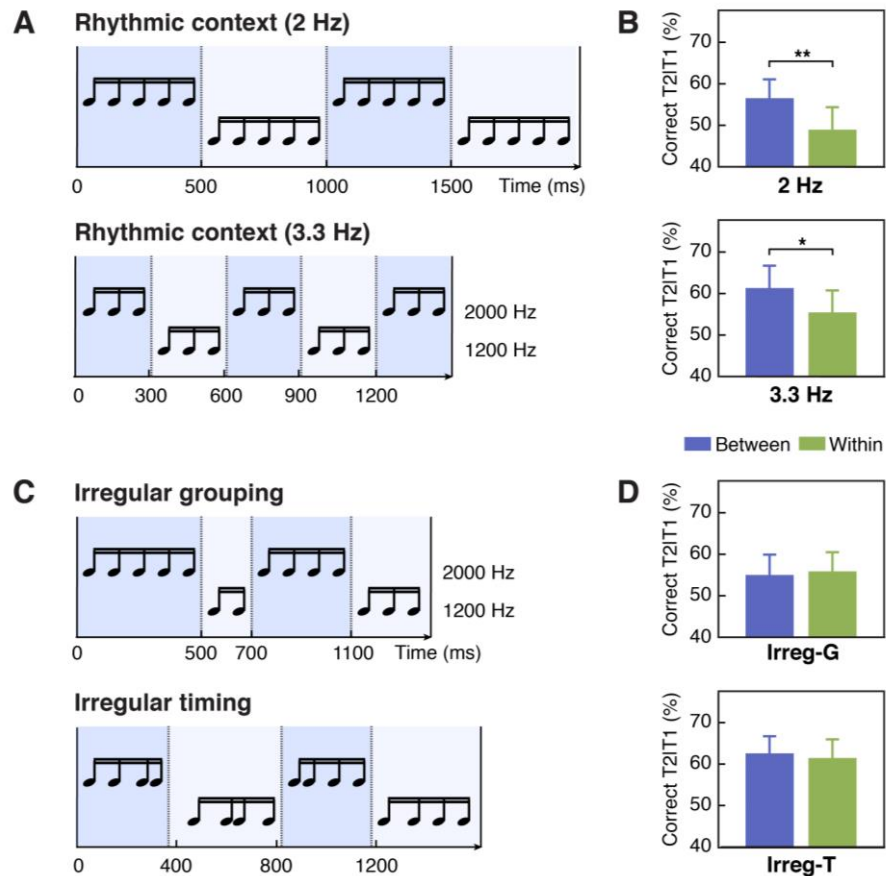
Fig. 2. Stimuli and results for Experiments 1c, 1d & 1e. (A) Contextual tone sequences with pitch changed every 5 tones (2 Hz, upper) and every 3 tones (3.3 Hz, lower) in Experiment 1c. (B) T2 performance in short-SOA conditions for 2-Hz(upper) and 3.3-Hz (lower) sequence in Experiment 1c. (C) The auditory context was grouped irregularly into four chunks with different numbers of tones (G-irregular) in Experiment 1d (upper) and into four regular chunks (four tones in each) but with irregular onset timing (T-irregular) in Experiment 1e (lower). (D) T2 performance in Experiment 1d (upper) and 1e (lower). Error bars represent 1 SEM; * $p<0.05$, ** $p<0.01$.

Figure 3
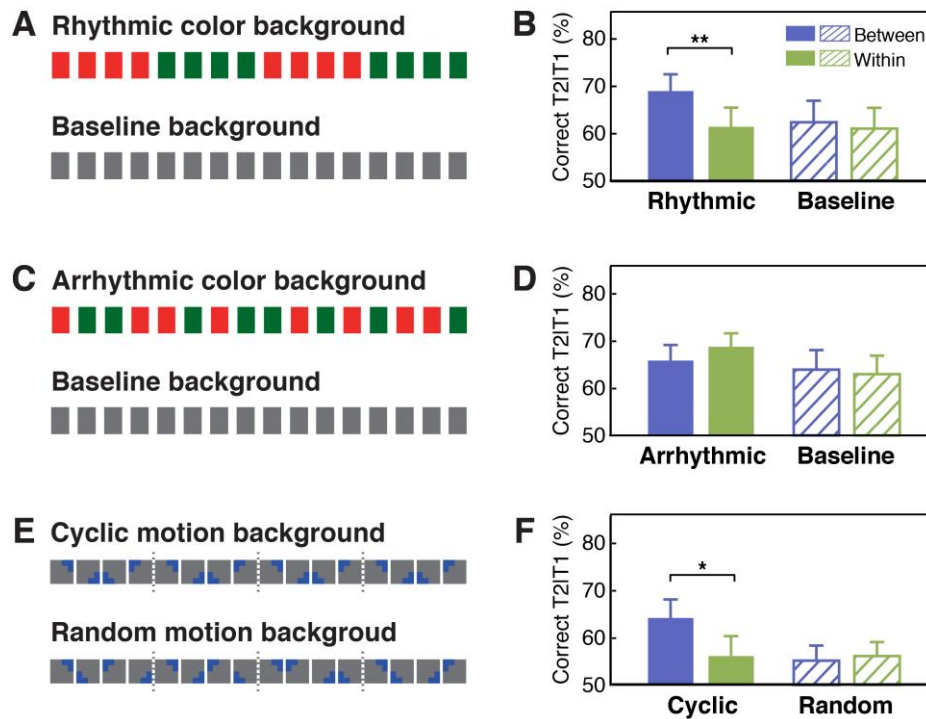
Fig. 3. Stimuli and results for Experiments 2 and 3 using the visual contexts. (A) The visual context with or without periodic changes in the background color and (B) the T2 performance in Experiment 2a. (C) The visual context with or without the background color changed irregularly and (D) the T2 performance in Experiment 2b. (E) Contextual rhythms defined by cyclic/random motion at a constant speed and (F) the T2 performance in Experiment 3. Error bars represent 1 SEM; * $p<0.05$, ** $p<0.01$.

967   **Figure 4**
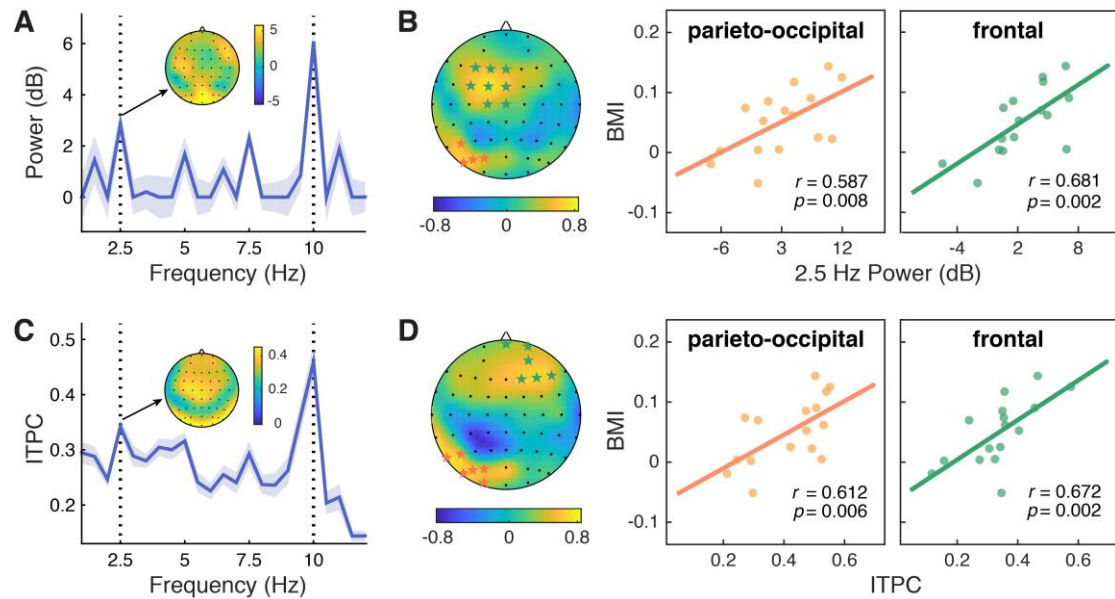
968   **Fig. 4.** Neural entrainment to contextual rhythms and its correlation with the attentional
969   modulation effect. (A) The power spectrum of EEG signals averaged across all epochs and
970   channels. For each frequency, power was normalized by subtracting the mean power of
971   the two nearest neighboring frequencies from the power of the center frequency. Shaded
972   areas indicate standard errors of the mean. (B) The 2.5-Hz power entrainment effect in
973   the parieto-occipital cluster (middle, in orange) and the frontal cluster (right, in green),
974   as in indicated in the scalp topographic map (left), significantly correlated with the
975   behavioral modulation index (BMI). (C & D) Analysis of inter-trial phase coherence (ITPC)
976   results yielded similar patterns to that for power.
977

978 **Figure 5**
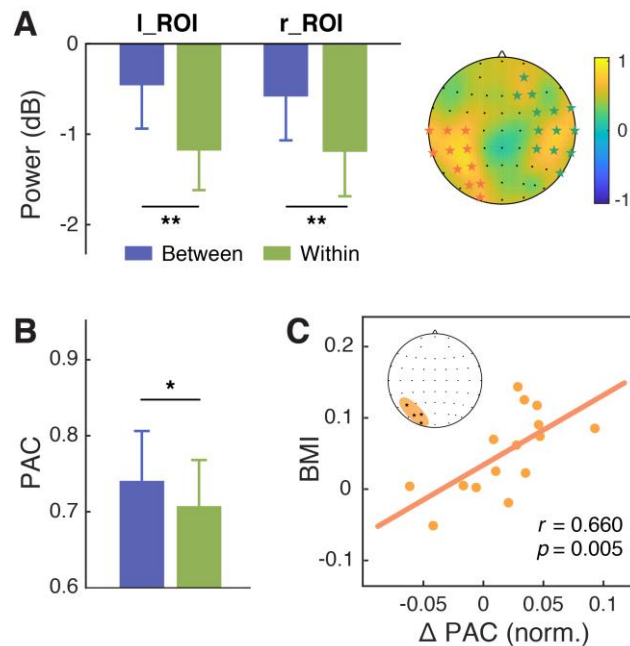
979 **Fig. 5.** Modulation effect of the alpha power and its coupling with the delta phase. (A) T2-
980 related alpha power averaged within the time window of 0–100 ms relative to the T2
981 onset was significantly higher in the between-cycle condition than in the within-cycle
982 condition in a left parieto-occipital cluster (starred in orange) and a right-lateralized
983 cluster (starred in green). (B) The modulation index of phase-amplitude coupling (PAC)
984 between the delta and alpha bands was higher for the between-cycle condition than for
985 the within-cycle condition, and (C) the difference in normalized PAC strength could
986 predict the BMI across individuals. Shadowed area in the topographic plot indicates the
987 cluster showing significant behavioral relevance in both delta- and alpha-band activities.
988 Error bars represent 1 SEM; * $p<0.05$, ** $p<0.01$.